Journal of New Sciences

Experimental and theoretical investigation of drying behavior of garlic in infrared dryer

J. LITAIEM [1,2] ; **D. MIHOUBI** [3] ; **A. TOUIL**[1] ; **F. ZAGROUBA** [1]

[1] High Institute of Sciences and Environmental Technology Borj-Cédria.
[2] National Agronomical Institute of Tunisia.
[3] Thermal Processing Laboratory, Research and Technology Centre of Energy, Hammam-Lif, Tunisia

* Auteur correspondent: jihene.litaiem@yahoo.fr

Abstract- The thin-layer infrared drying behavior of garlic was experimentally investigated in the temperature range from 40°C to 70°C. The drying rate was found to increase with temperature, thus reducing the total drying time. Based on the simultaneous heat and mass transfer, a mathematical model was proposed for predicting the temperature and moisture distribution in the drying sample, applying Fick diffusion equation. A numerical solution was developed for the proposed model using an implicit finite difference method in bi-dimensional system. The main objective of this paper is to formulate an accurate transport model analyzing the simultaneous transfers of heat and mass within garlic slices. The suggested model takes into account garlic deformation and determines the time and space evolutions of moisture, temperature and solid displacement within garlic slices.

Key Words: Garlic, Infrared Drying, Heat and mass transfer, modelisation

1. Introduction

Garlic (*Allium sativum L.*) has been used not only as a spice and a flavoring agent for food but also as a supplement for medicinal effects, such as antimicrobial, antithrombotic, antioxidant and anticancer activities (Lawson and Wang, 2001). Garlic powder, one of the most popular commercial garlic products, can be produced by drying garlic cloves or slices. The dried samples are then pulverized into powder. Several types of dryers have been developed in an aim to respond to the requirements of quality and energy efficiency. Therefore, execution of this process with high thermal efficiency is of great importance. Various methods of drying garlic have been developed and each method has its own characteristics.

Ratti et al. (2007) studied the freeze-dried garlic slices. However, this drying method is rather expensive. Hot-air drying is another method commonly used for drying garlic slices (Cui et al., 2003; Ratti et al., 2007). This drying method is much less expensive than freeze drying, however it may be noted that convective heating achieves a lower rate of heat transfer than other heating methods. It also requires increased product exposure time and has as slower start-up/cool down than other heating methods. In addition the airflow in convective dryers can disturb or contaminate the product.(Litzler M, 2006). Therefore innovative drying methods have been recently developed. Sharma et al., 2006 have studied the microwave-convective drying process of garlic cloves at various air temperature, air velocities and microwave power levels. Méndez Lagunas and Castaigne, 2008 have studied the effects of temperature cycling and constant temperature drying on the preservation of the quality potential in garlic. On the aim to preserves the allicin potential in garlic slices, Rahman et al., 2009 have investigated the drying slices of garlic in air, vacuum, and nitrogen atmosphere. Thuwapanichayanan et al., 2014 tested a novel drying method which is a far-infrared radiation-assisted heat pump, for drying chopped garlic and compared with conventional hot-air drying.

Although these experimental investigations have been done on the drying of garlic, there is a little detailed analysis on mathematical modeling of simultaneous heat and mass transfer in drying systems. Abbasi Souraki and Mowla 2008; Thuwapanichayanan.et al., 2014, have studied mass and heat transfer within garlic slices. Their works were based on developed a mathematical model without

Litaiem et al. (2015) / Journal of new sciences, Agriculture and Biotechnology, JS-INAT(6), 861-867

861

taking shrinkage into account during drying. Volume changes inside the dried material during drying were considered negligible, and up until now there is no theoretical work has developed a coupled heat and mass transfer model to describe the drying of garlic sample with considering product shrinkage during drying. Therefore, the objective of this work was to study the two-dimensional heat and mass transfers which reflect the real physical phenomena occurring in dried garlic. A model describing the evolution of the local variables inside the garlic during the infrared drying such as moisture, garlic temperature and garlic displacement was established. This model was based on some simple assumptions, on conservation equations for heat and mass transfers and appropriate initial and boundary conditions. The shrinkage of the material was also included by establishing an empiric relationship between material displacement and moisture loss.

2. Shrinking factor

The equilibrium relation between the apparent density of the product and its moisture content was investigated by means of an apparatus based on Archimedes's law. The volume of the sample is determined by measuring the difference in weight of that sample above and under water. The sample is coated with paraffin to prevent the uptake of water. The sample used in the experiences was a layer cutted off from the dried garlic slices"Figure 1"

According to Mihoubi et al., (2002), the variation of the specific volume (m^3/kg) with the water content was proposed:

$$\frac{\vartheta}{\vartheta_0} = 1 + \beta W \qquad (1)$$

Where β is the shrinkage coefficient, ϑ the specific volume at material moisture content W, and ϑ_0 the specific volume at material moisture content W = 0.

Thus: $\rho = \frac{\rho_0}{1+\beta W} \qquad (2)$

3. Mathematical modeling

The studied system is treated as a porous cylindrical material (Figure 1). The porous medium is a deformable product composed of a solid phase, and a liquid phase (water). The proposed mathematical model describes the mass and heat transfers in product garlic sample during drying. These two transfers' phenomena are associated with a shrinkage behavior.

The exchange surfaces are driven by convective flux and radiative flux, the studied system is presented in Figure 1.
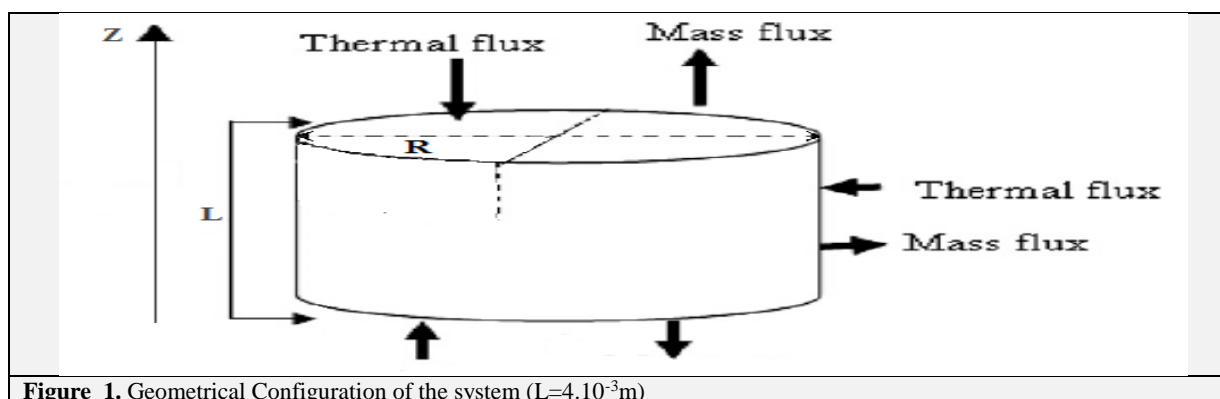
Figure 1. Geometrical Configuration of the system (L=4.10^{-3}m)

Several simplifying assumptions were made in order to obtain a closed set of governing macroscopic equations:

   (a) A garlic cylindrical geometry by considering an axis-symmetry ;
   (b) Garlic is a solid, isotropic porous medium ;
   (c) Garlic is inert, i.e. without any chemical energy consuming or generating reactions ;
   (d) Moisture could be present in the garlic in a free or bound state ;
   (e) Initially the moisture and the temperature of garlic are uniform ;

$$t = 0, w = \overrightarrow{w_0} , \quad T = \overrightarrow{T_0}$$

   (f) The moisture content and temperature profile are non uniform at any time of drying ;

$$\text{For } r = 0 \; ; \frac{\partial W}{\partial r} = 0 \; ; \quad \frac{\partial T}{\partial r} = 0$$

$$\text{For } z = 0 \; ; \frac{\partial W}{\partial z} = 0 \; ; \quad \frac{\partial T}{\partial z} = 0$$

(g) The stress has no reciprocal influence on heat and moisture transferred (Ponsart et al., 2003) ;

(h) The material shrinks according to the loss of water without generating any gas phase or porosity within the product (Stamatopoulos, 1986)

(i) Heat and mass transfers are governed by diffusion within the product and by radiation and convection between the material and the environment air.

(j) The boundary conditions for the moisture and the temperature transfers stimulate the symmetry of the moisture and temperature potentials at the middle point of the porous cylinder.

Considering the assumptions, the macroscopic equations governing heat and mass transfers in the cylindrical porous slab are summarized as follows:

3.1. Mass conservation

Mass balance equations could be written in an Eulerian reference, in which the product has shrinked.

Solid   : $$\frac{\partial \rho_s}{\partial t} + \nabla.\left(\rho_s \vec{\vartheta}_s\right) = 0 \tag{3}$$

Liquid : $$\frac{\partial \rho_l}{\partial t} + \nabla.\left(\rho_l \vec{\vartheta}_l\right) = 0 \tag{4}$$

Where ρ_i is the apparent density of the phase i, and $\vec{\vartheta}_i$ its velocity : i= « s » and « l » for solid and liquid, respectively.

The liquid flux is the sum of a diffusive flux and a convective flux.

$$\rho_l \vec{\vartheta}_l = -\rho D_{eff} \nabla \left(\frac{\rho_l}{\rho}\right) + \rho_l \vec{\vartheta} \tag{5}$$

Where ϑ is the barycentric volocity system.

For a product composed exclusively of liquid and solid and undergoing an ideal shrinkage, we can write the following relationships (Ketelaars, 1993):

$$\vec{\vartheta} = \frac{\rho_l \vec{\vartheta}_l + \rho_s \vec{\vartheta}_s}{\rho} \tag{6} \; ; \qquad W = \frac{\rho_l}{\rho_s} \tag{7}$$

$$\rho = \rho_l + \rho_s \tag{8} \; ; \qquad \rho_s = \frac{\rho_{ss}}{1 + \beta W} \tag{9}$$

Where ρ_{ss} is the solid intrinsic density and β is the volume shrinkage coefficient and is defined as :

$$\beta = \frac{V_{(W)} - V_s}{w V_s} \tag{10}$$

Where V is the apparent volume of the sample.

Using the previous equations, the moisture distribution is written as follows:

$$\rho_s \left(\frac{\partial w}{\partial t} + \overrightarrow{\vartheta_s}.\nabla(w)\right) = \nabla.\left(\rho \frac{D_{eff}}{(1+w)} \nabla(w)\right) \tag{11}$$

In a cylinder shape where the mass transfer was radial and longitudinal:

$$\rho \left(\frac{\partial w}{\partial t} + \left(\vartheta_r \frac{\partial w}{\partial r} + \vartheta_z \frac{\partial w}{\partial z}\right)\right) = \frac{1}{r} \left\{\frac{\partial}{\partial r}\left(\frac{\rho}{(1+w)} D_r \frac{\partial w}{\partial r}\right) + \frac{\partial}{\partial z}\left(\frac{\rho}{(1+w)} D_z \frac{\partial w}{\partial z}\right)\right\} \tag{12}$$

Where ϑ_r and ϑ_z are respectively the radial and the longitudinal components of the volocity.

3.2. Energy conservation

According to the hypothesis (i) that the evaporation occurs only at the surface level of the product, the internal heat transfer obeys to the Fourier's law with an apparent conductivity coefficient depending on the moisture content and could be expressed as follows :

$$\frac{\partial(\rho C_p T)}{\partial t} + \vec{V_s}.\overrightarrow{grad}\left(\rho c_p T\right) = div\left(k \overrightarrow{grad}(T)\right). \tag{13}$$

In a cylinder shape where the heat transfer was radial and longitudinal Eq. (13) becomes

$$\frac{\partial(\rho C_p T)}{\partial t} + \left(V_r \frac{\partial(\rho C_p T)}{\partial r} + V_z \frac{\partial(\rho C_p T)}{\partial z}\right) = \frac{1}{r}\left\{\frac{\partial}{\partial r}\left(kr \frac{\partial T}{\partial r}\right) + \frac{\partial}{\partial z}\left(k \frac{\partial T}{\partial z}\right)\right\} \tag{14}$$

(Z=L) : On the cylinder surface, the product exchanged heat by both convection and radiation. Then, the energy balance equation could be written :

$$(h(T_a - T_{sur}) + Q_{abs}) = \left(\dot{m} L_v(T_{surf}) + k \frac{\partial T}{\partial z}\right) \tag{15}$$

Where : $h(T_a - T_{sur})$: is heat density exchanged by convection ;

Q_{abs} : is the infrared flux density absorbed at the surface of the sample

$\dot{m}\,L_v$: is the heat density due to the moisture vaporization ;

$k\dfrac{\partial T}{\partial z}$: is the flux density transmitted by conduction in the product.

3.3. Principe of radiative heating

Infrared heating is the transfer of thermal energy in the form of electromagnetic waves. True infrared heat should have one common characteristic: that the transfer of heat is emitted or radiated from the heated object or substance. The source emits radiation at a peak wavelength towards an object. The object can absorb the radiation at some wavelength, reflect radiation at other wavelengths, and re-radiate wavelengths. It is the absorbed radiation that creates the heat within the object. The material molecules absorb the radiation of certain wavelengths and energy, causing excited vibration and the electromagnetic wave energy is absorbed directly by the dried product with reduced energy loss (Wango et al., 2011). Two factors, attenuators of infrared exchanges, intervene to describe exchanges between transmitters and real products :

- The form factor, related to the geometry of the transmitter and receiver, which allows specifying the percentage of emitted infrared flux by the source that actually reaches the product to be treated.
- The absorption factor that defines the part of the infrared flux effectively transformed into energy in the product.

The infrared flux density absorbed at the sample surface is expressed below:

$$Q_{abs} = \alpha_a . Q_{ray} \tag{16}$$

Where Q_{ray} is the power density radiated by the emitter and α_a is the absorption coefficient=1.

3.4. Resolution

To solve the set of equations, we have used the commercial finite element solver COMSOL 5. An Arbitrary Lagrangian-Eulerian (ALE) description was adopted. It is worthwhile to remark that the ALE method can be considered as « intermediate » between the Lagrangian and Eulerian approaches since it combines the best features of both of them and allows describing moving boundaries without the need for the mesh movement to follow the material. This resolution allows consideration of a drying process of a shrinking body. The shrinkage factor, the initial and equilibrium moisture content and the bulk density were measured experimentally (Table 2). The other physical properties of garlic taken from literature and injected in the model are reported in Table1.

Table 1. Input parameters used for simulation		
Property	**Expression**	**Références**
Density ρ (kg/m³)	$\rho = 1338\dfrac{(1+W)}{(1+0,6757W)}$	Our Results
Liquid and Solid Specific heat (kJ/kg⁻¹K⁻¹)	C_p^s =3000 C_p^l =4182	(Madamba et al., 2007)
Equilibrium moisture content W_{eq} (kg/kg d.b)	$W_{eq} = \dfrac{C.K.a_w.W_m}{(1-K.a_w).[1+(C-1).K.a_w]}$ C= 1.43; K=1.026 ; W_m=0,063	Our Results
Effective diffusion coefficient : D_{eff} (m².s⁻¹)	$D_{eff} = 1.1\,.10^{-4}exp\left(\dfrac{-334317}{R.T_{abs}}\right)$	(Rasouli et al., 2011)
Thermal conductivity : λ_{eff} (W/m.K)	0.4	(Madamba et al., 2007)

Journal of New Sciences

4. Results and discussion

Figure 2 shows the experimental variation of the specific volume versus the average moisture content of garlic. The specific volume varies linearly versus garlic moisture content. This linear evolution corresponds to a total shrinkage (Eq. (1)), which means that the volume loss is equal to the volume of removed moisture. The shrinkage coefficient of garlic, β, determined from the slope (Figure 2), is about *0.6819*. Results of the experimental fit of the specific volume and the bulk density are given in Table 2 with $R^2 = 0.99$.

| Table 2 : Experimental fit results of garlic shrinkage and bulk density variations.					
ϑ	ϑ_0	*Shrinkage*	β	$\rho°_s$ *(kg/m³)*	ρ *(kg/m³)*
0,6819W + 0,2604	*0,2604*	0,6819W	*0,6819*	*1338*	$\rho = 1338 \dfrac{(1 + W)}{(1 + 0,6757W)}$

The solid displacement varies linearly with drying time and reaches a constant value at the end of drying (≈4000 s) when the rate of dehydration becomes small. This result is concordant with the linear variation of the specific sample volume shown in Figure 2.
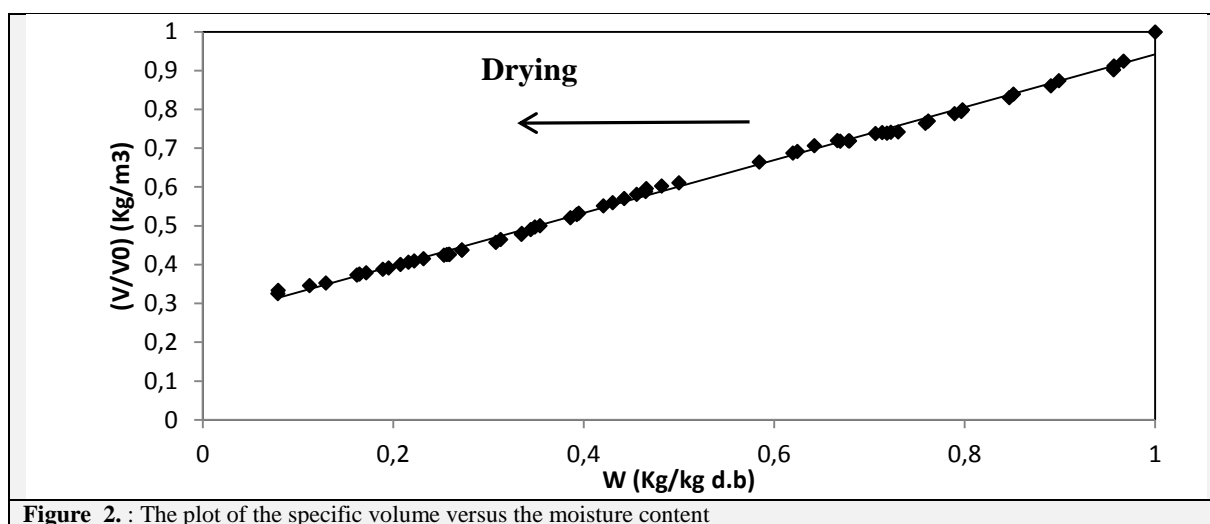

Figure 2. : The plot of the specific volume versus the moisture content

Figure 3. Shows the evolution of the average temperature, shrinkage and moisture of garlic sample during drying time, obtained for drying kinetics simulated at 70°C with $Q_{ray} = 600$ W/m². After the initial drying period, the evaporation was controlled by moisture diffusion rate through the product. During this period of drying, the temperature of the product was constant and approached the wet-bulb temperature. Thereafter as the moisture flux decreased with drying time. The energy transferred to the garlic product by radiation becomes sufficient to supply heat of moisture vaporization and to heat up the product. Consequently, the product temperature increased exponentially. Then, the moisture field took a nest shape. At the end of dehydration process, the moisture field flattened and tended to low moisture levels until reaching the equilibrium moisture content of garlic. The temperatures at the surface of garlic were higher than the drying air temperature at the end of drying.

Figure 4. shows the spatial distribution of moisture content of garlic obtained at 3000s instant drying time and at 70°C drying temperature. The moisture gradient decreased in the same sense from the inside to outside (radial and longitudinal) of the garlic sample. However, the moisture gradient intensity changed with different sides of the studied medium. This difference is related to the considered mass transfer and corresponding surface exchange. In fact, the radial surface is greater than the longitudinal one and the corresponding radiation are different.

.

Journal of New Sciences
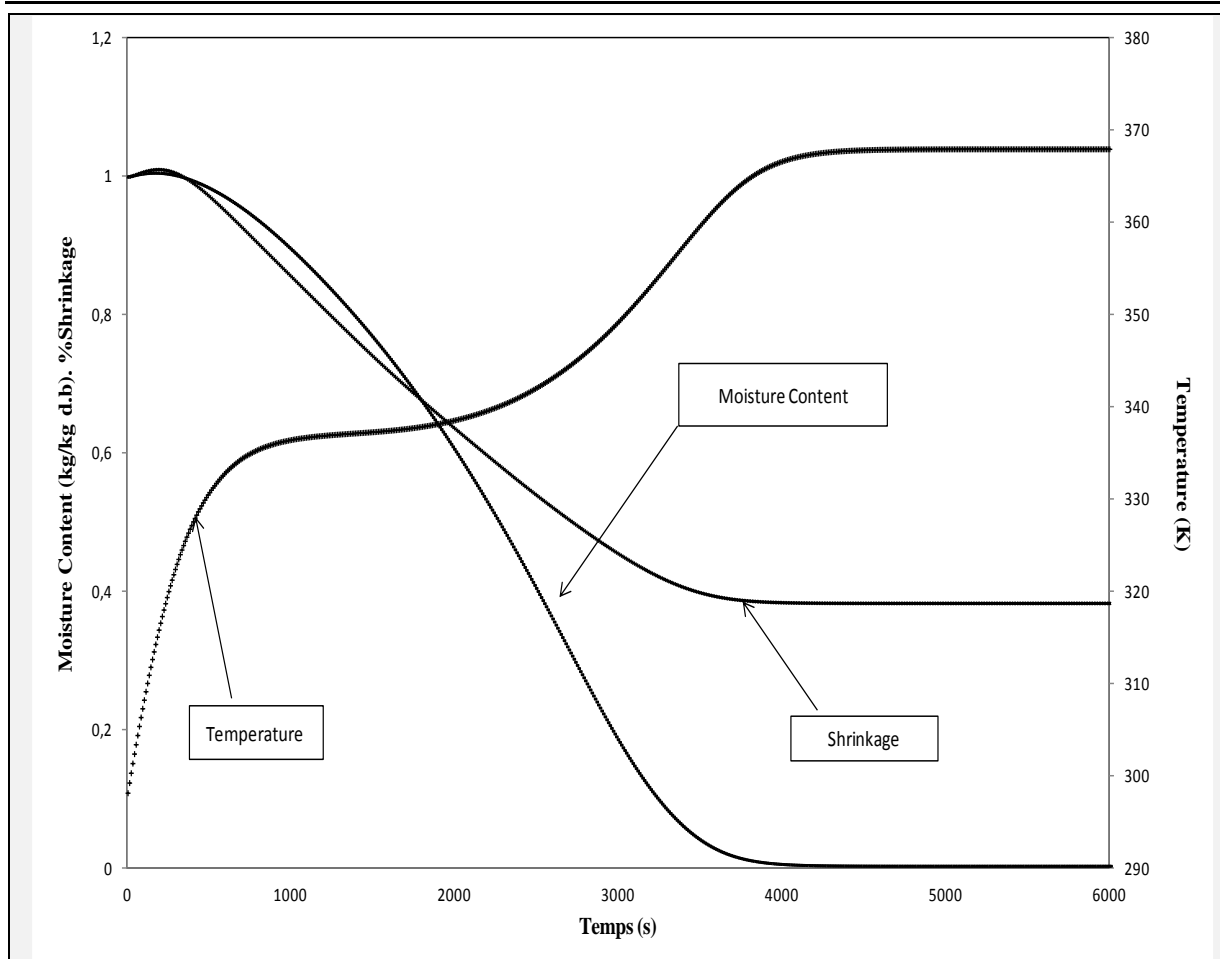
Figure 3. Variations of average moisture content, shrinkage and surface temperature of the garlic sample versus time.
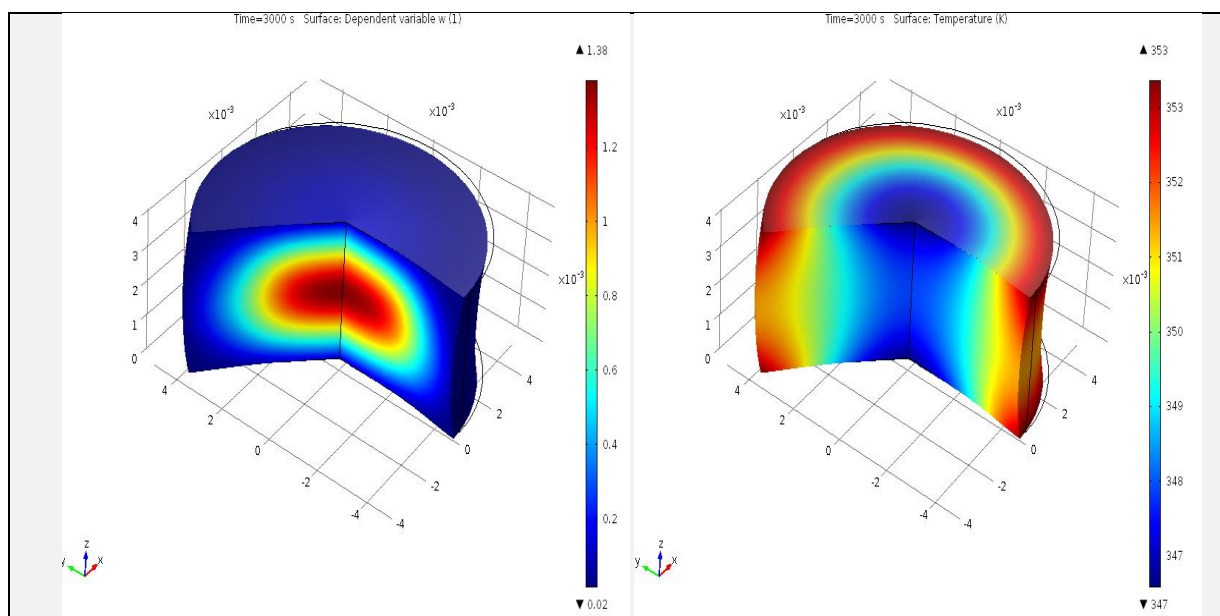
Figure 4. Moisture distribution within the garlic thin-layers at t=3000s ; T =70∘C, Q_{ray} =600 W/m². | **Figure 5.** Temperature distribution within the garlic thin-layers at t=3000s; T=70°C, Q_{ray} =600 W/m²

Figure 5. shows the temperature distribution of garlic obtained at the same previous drying conditions (t=3000s; Ta=70°C and Q_{ray} =600 W/m²). Unlike the moisture gradient, the temperature distribution of product increased in radial sense from inside to outside, but it is seems constant in the longitudinal sense. This clearly gives an indication that the product temperature depends on moisture diffusivity,

which varies inside the product and affects the rate of moisture diffusion. The low temperature gradients in the longitudinal sense are certainly due to the small thickness (4.10^{-3}m) compared to the cylindrical diameter of sample (7.10^{-3}m). The garlic surface in direct contact to the heated air and submitted to the radiative flux reaches quickly a higher temperature than the center of the product. Thus heat transfers from the surface to the interior of garlic sample.

Figure 4. and Figure 5. shows the variation of the solid displacement versus distribution of moisture content and temperature respectively. The center section of the sample ($0<z < L$; $0<r<R$) shrank more than the exterior section of the product ($z = L$). The shrinking is higher on the radial direction than the longitudinal direction. The solid displacement was not uniform within the sample because of the internal gradient of moisture content and temperature generated during drying.

5. Conclusion.

A mathematical model, describing heat and mass transfers and taking into account product deformation, was suggested. The numerical solution of temperature and moisture content distributions inside the product subjected to infrared drying is presented. It is found that the temperature rises rapidly in the early drying period and as the drying process progresses, the rise of temperature attains almost steady. The moisture gradient is higher in the early drying period and as drying progresses, the moisture gradient remains almost steady. The developed model provides spatio-temporal distributions of moisture content, temperature and solid displacement within garlic thin-layers. Consequently, the model could be suggested as a mathematical tool providing useful data concerning infarred drying of other food products.

6. References

Abbasi Souraki, B.,Mowla, D (2008) Experimental and theoretical investigation of drying behaviour of garlic in an inert medium fluidized bed assisted by microwave. Journal of Food Engineering 88 : 438–449.

Cui, Z.W., Xu, S.Y., Sun, D.W (2003) Dehydration of garlic slices by combined microwave-vacuum and air drying. Drying Technol. 21, 1173–1184.

Ketelaars AAJ (1993) Drying deformable media, kinetics, shrinkage and stress. University of Endhoven.

Madamba. P.S., Driscoll, R.H., Buckle, K.A (2007) Models for the specific heat and thermal conductivity of garlic. Drying technology:An international Journal13, 295-317.

Mihoubi, D., Zagrouba, F., Ben Amor, M., & Bellagi, A (2002) Study of process of clay drying: Part I. Physico-chemical characterisation of material. Drying Technology, 2, 465–487

Lawson, L.D., Wang, Z.J (2001) Low allicin release from garlic supplements: a major problem due to the sensitivities of alliinase activity. J. Agric. Food Chem. 49, 2592–2599.

Litzler M. (2006) Understanding drying methods

Méndez Lagunas, L.L., Castaigne, F (2008) Effect of temperature cycling on allinase activity in garlic. Food Chem. 111, 56–60.

Ponsart, G., Vasseur., J., Frias, M., Duquenoy, A., Méot, J.M (2003) Modelling of stress due to shrinkage during drying of spaghetti, J. Food Eng. 57, 277–285.

Rahman, M.S., Al-Shamsi, Q.H., Bengtsson, G.B., Sablani, S.S., Al-Alawi (2009) Drying kinetics and allicin potential in garlic slices during different methods of drying. Drying Technol. 27, 467–477.

Rasouli, M., Seiiedlou, S., Ghasemzadeh, H, R., Nalbandi, H (2011) Influence of drying conditions on the effective moisture diffusivity and energy of activation during the hot air drying of garlic. Aust Jour Agric Eng. 2, 96-101.

Ratti, C., Farias, M.A., Lagunas, L.M., Makhlouf, J (2007) Drying of garlic (Allium sativum) and its effect on allicin retention. Drying Technol. 25, 349–356.

Sharma, G.P., Prasad, S (2006) Optimisation of process parameters for microwave drying of garlic cloves. J. Food Eng. 75, 441–446.

Stamatopoulos, (1986) Contribution à l'étude expérimentale et théorique du séchage des pâtes alimentaires, Thèse de l'université des sciences et Techniques du Languedoc.

Thuwapanichayanan, R., Prachayawarakorn, S., Soponronnarit, S (2014) Heat and moisture transport behaviour and quality of chopped garlic undergoing different drying methods. J. Food Eng. 136, 34-41.

Wango P, Siriamornpun S, Meeso N (2011) Improvement of quality and antioxidant properties of dried mulberry leaves with combined far-infrared radiation and air convection in Thai tea process. Food Bioprod Process, 89:22–30.